Supporting Information

A Mathematical Analysis of Carbon Fixing Materials that Grow, Reinforce, and Self-Heal from Atmospheric Carbon Dioxide

Dorsa Parviz†, Daniel James Lundberg†, Seonyeon Kwak, Hyunah Kim, Michael S. Strano*

Department of Chemical Engineering, Massachusetts Institute of Technology, Cambridge MA, 02139 USA.
**Corresponding author: strano@mit.edu*
†These authors contributed equally to this work.

Kinetic modeling of CO_2 Photocatalytic Reduction:

Reaction networks including formaldehyde (RF in the manuscript), carbene (RC in the manuscript), and combination of both pathways, with and without reversible reactions, were fitted against the experimental data assuming two-electron transfer steps for each network to avoid overparameterization. To develop the kinetic model for each network, surface reactions were considered the rate-limiting steps, assuming no limitations in mass transfer to/from catalyst surface and no limitation in electron transfer from bulk of catalyst to the reactants. Additionally, adsorption/desorption of reagents, intermediates, and products were assumed to happen fast. Since CO_2 and hydrogen evolution (water oxidation reaction) data was not reported in this study, we refrained from using a surface Langmuir-Hinshelwood model that will include a variable proton concentration profile over time and instead used bulk product concentration in the first order rate expressions to avoid overfitting the data and over parameterizing the kinetic model. Also, we assumed abundant protons are provided in the system through the water oxidation reaction such that its concentration can be considered constant. Last, the concentration of CO_2 in the liquid phase was calculated using Henry's law from an atmospheric concentration of 400 ppm.

Fitting of various kinetic models to the experimental data and parameter estimation was performed in a single step using multi-objective optimization. Individual reaction rates were expressed as functions of the chemical concentrations and expressions for concentration profiles of reactant and products were defined. Parameters were constrained in a range of 10^{-10} to 1 (1/s) and fitting was performed by simultaneous calculation and minimization of the following objective function (OF) using the ordinary least square (OLS) difference between the values of the experimental concentration of each product C_i^{exp} and the modeled one $C_{i,k}^{model}$. The optimization algorithm was coded in MATLAB.

$$OF(k)_{i=CO_2,\ HCOOH,\ CO,\ HCHO,\ CH_3OH,\ CH_4} = \sum_{k=1}^{N_{exp}} \left(C_i^{exp} - C_{i,k}^{model}\right)^2$$

Sensitivity Analysis of CO_2 reduction kinetic Model:

Local sensitivity analysis evaluates the influence of parameter p on a model output, $y_i\ (t,p)$ with respect to changes in the a single parameter input. The sensitivity indices are defined as first-order partial derivatives of the model output, y_i with respect to the parameter p_j around an optimal parameter value of $p = p^*$:

$$S_{ij}(t) = \frac{\partial y_i(t,p)}{\partial p_j}$$

For a system of ODES, $f\ (y,p)$, sensitivity indices can be calculated by the direct differential method:

$$\frac{d}{dt}\frac{\partial y}{\partial p_j} = \frac{\partial f}{\partial y}\frac{\partial y}{\partial p_j} + \frac{\partial f}{\partial p_j} = J * S_j + F_j$$

in which, J is the Jacobian matrix of the system, S_j is the sensitivity indices vector, and F_j is the function-parameter derivatives vector.[1, 2]

Here, we use the ODE system of equations obtained as the best fitting model for CO_2 reduction reaction and evaluate the sensitivity indices with respect to rate constants k_1-k_6 around their optimal values reported in **Table 1** of the manuscript. Finally, the normalized sensitivity indices are calculated as below:

$$S_{ij}(t) = \frac{\partial y_i(t,p)}{\partial p_j} . \frac{p_j^*}{y_i(t,p^*)}$$

Kinetic Modeling of Formaldehyde Trimerization:

The reversible rate constants of reaction 7-9 at 371 K were calculated by extrapolating the rate constants reported by Winkelman et al. at 293-333 K (R7, Eq15-16) and Ott et al. at 293-323 (R8-R9, Eq16-18),[3, 4] the forward reaction rate constants were calculated using the reverse rate constants and the equilibrium constants reported by Winkelman et al. and Kuhnert et al. at 371 K.[3, 5] The rate constants for the cyclization reaction (R10, Eq18-19) were obtained by fitting experimental data of trioxane formation reported by Yin et al. at 371 K to the above kinetic model.[6] The fitting of kinetic model to experimental data was performed using similar least square minimization strategy described for the CO_2 photocatalytic reduction. The rate constants obtained at this temperature were close to values obtained by Zhang et al., although they used a different reaction mechanism including the side reactions of formaldehyde producing formic acid and methanol as byproducts.[7] Knowing the rate constants of the cyclization reaction at 371 K, we used the activation energy estimated for this reaction using Density Functional theory (DFT) by Kua et al. (22.7 kcal/mol for forward reaction and 21.5 kcal/mol for reverse reaction) to obtain the rate constants at the room temperature by applying the Arrhenius law.[8]

Kinetic Modeling of Trioxane Polymerization:

The trioxane consumption expression (R11, Eq20) was fitted to the data provided in literature for trioxane polymerization at 30 C using similar least square minimization strategy described for the CO_2 photocatalytic reduction.[9]

Overall POM growth rate calculations:

The rate constants indicated in Table 1 of the manuscript were used to evaluate the rate of production of POM under continuous supply of CO_2 (400 ppm) over time. The term for initiator concentration in eq. 14 is substituted with a variable initiator concentration [I] = $10^{-2}[(CH_2O)_3]$ to maintain the realistic ratio of the monomer to initiator at any time during the polymerization reaction in the compartmental catalytic unit. To capture the polymer production from trioxane conversion, any byproduct formation is neglected, and the final polymer is taken to be a chain of 500 repeat units, equivalent to a molecular weight (Mw) of ~ 15,000 g/mol (averaged over the literature data for POM molecular weight obtained at various synthesis conditions.[10] Any discussion or incorporation of a molecular weight distribution of the products is beyond the scope of this work. Relative improvement over kinetics of each reaction unit was obtained by multiplying the rate constant of each unit by a constant factor.

Amine Adsorption Rate:

Here, an aqueous solution of monoethanolamine is taken as a CO_2 adsorbent. To calculate a appropriate pseudo-first order rate constant for this adsorbent, kinetic data of CO_2 adsorption into aqueous solutions of 3% sodium hydroxide is taken from Yoo *et al.*[11] This adsorption data was fit to the pseud-first order model of adsorption (Eq.(1)) using Solver in Microsoft Excel. A value for the total adsorption capacity was taken as the maximum concentration of dissolved CO_2 attained in the experiments at 0.726 mole CO_2 L^{-1}. The fit pseudo-first order rate constant was at a value of $7.62 \cdot 10^{-4}\, hr^{-1}$.

Table S1. A subset of the feasible one and two electron reaction steps for the photocatalytic reduction of CO_2 suggested in the literature based on theoretical calculations and or experimentally observed intermediates and products on various catalyst surfaces and reaction conditions.

	Reaction Steps	**Description**	**ref**
(1)	$CO_2 + e^- \rightarrow CO_2^-$		12-14
(2)	$CO_2^- + H^+ \rightarrow COOH$		12, 13
(3)	$COOH + e^- \rightarrow COOH^-$	Formate Formation	12, 14-16
(4)	$COOH^- + H^+ \rightarrow HCOOH$	Formic Acid Formation	14, 16
(5)	$HCOOH \rightarrow CO + H_2O$	Carbon Monoxide Formation	13, 15
(6)	$CO + e^- + H^+ \rightarrow CHO$		13, 15, 17, 18
(7)	$CHO + e^- + H^+ \rightarrow HCHO$	Formaldehyde Formation	13, 17, 18
(8)	$HCHO + e^- + H^+ \rightarrow CH_2OH$		17
(9)	$CH_2OH + e^- + H^+ \rightarrow CH_3OH$	Methanol Formation	17, 18
(10)	$CH_2OH \rightarrow CH + H_2O$		17
(11)	$CO + e^- + H^+ \rightarrow COH$		13, 15
(12)	$COH + e^- + H^+ \rightarrow C + H_2O$		13
(13)	$C + e^- + H^+ \rightarrow CH$		13
(14)	$CH + e^- + H^+ \rightarrow CH_2$		13, 17
(15)	$CH_2 + e^- + H^+ \rightarrow CH_3$		13, 17
(16)	$CH_3 + e^- + H^+ \rightarrow CH_4$	Methane Formation	13, 17
(17)	$CO + CHO \rightarrow COCHO$		19-21
(18)	$COCHO + e^- + H^+ \rightarrow OCHCHO$	Glyoxal Formation	19, 21
(19)	$OCHCHO + e^- + H^+ \rightarrow HOCHCHO$		19
(20)	$HOCHCHO + e^- + H^+ \rightarrow HOCH_2CHO$		19
(21)	$HOCH_2CHO + 2e^- + 2H^+ \rightarrow HOCH_2CH_2OH$	Ethylene Glycol Formation	21
(22)	$HOCH_2CH_2OH + 2e^- + 2H^+ \rightarrow CH_3CH_2OH + H_2O$	Ethanol Formation	19
(23)	$CO_2^- + CH_3 \rightarrow CH_3COO^-$	Acetate Formation	19
(24)	$CH_3COO^- + H^+ \rightarrow CH_3COOH$	Acetic acid Formation	19
(25)	$CH_3COOH + e^- + H^+ \rightarrow CH_3CO + H_2O$		19
(26)	$CH_3CO + e^- + H^+ \rightarrow CH_3CHO$	Acetaldehyde Formation	19
(27)	$CH_3CHO + 2e^- + 2H^+ \rightarrow C_2H_4 + H_2O$	Ethylene Formation	19

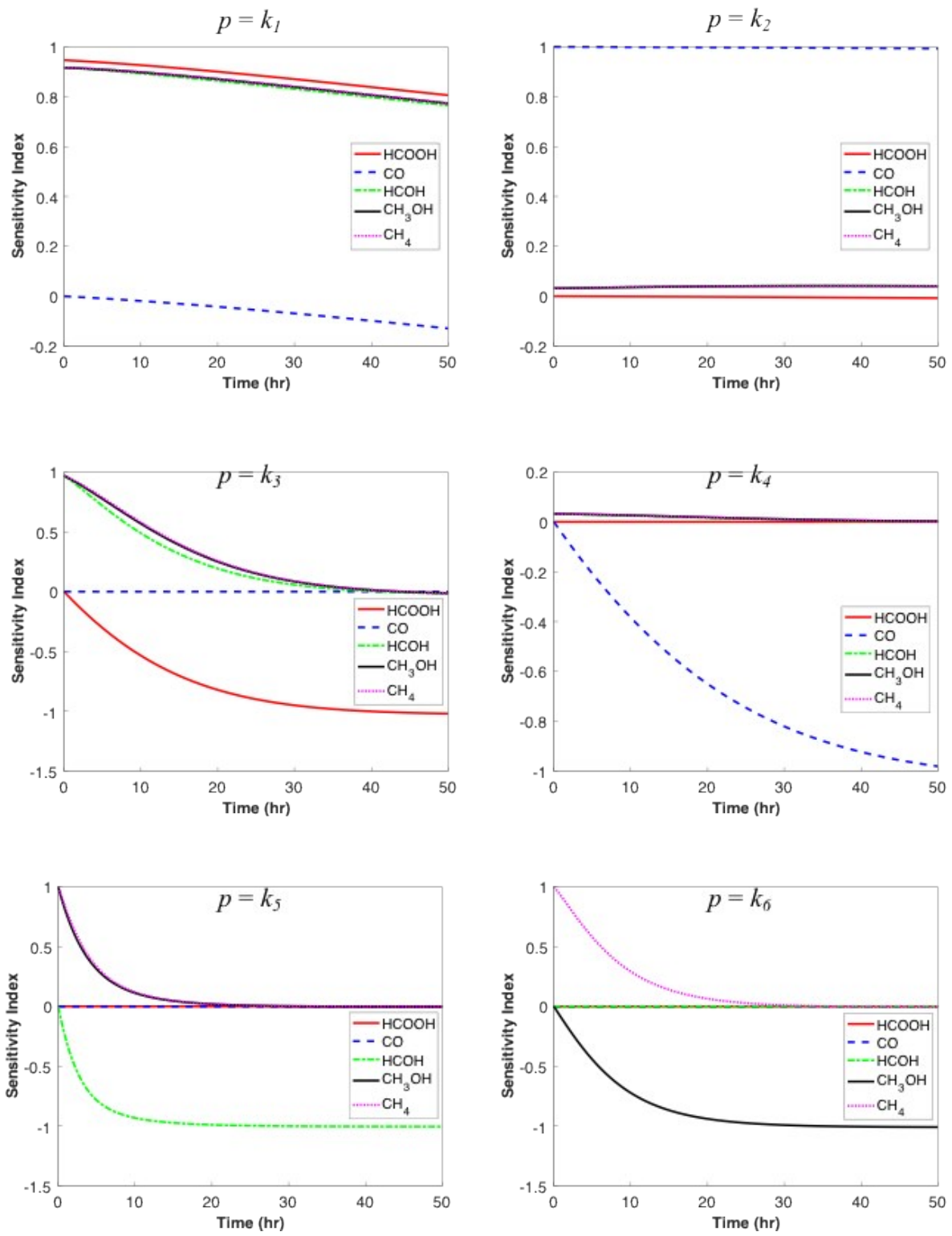

Figure S1. Local Sensitivity analysis of the CO_2 reduction reaction network (R1-R6 in the manuscript) for model rate constants k_1-k_6. Normalized sensitivity indices of reaction products with respect to k_1-k_6 around their optimal values reported in Table 1 are plotted over time.

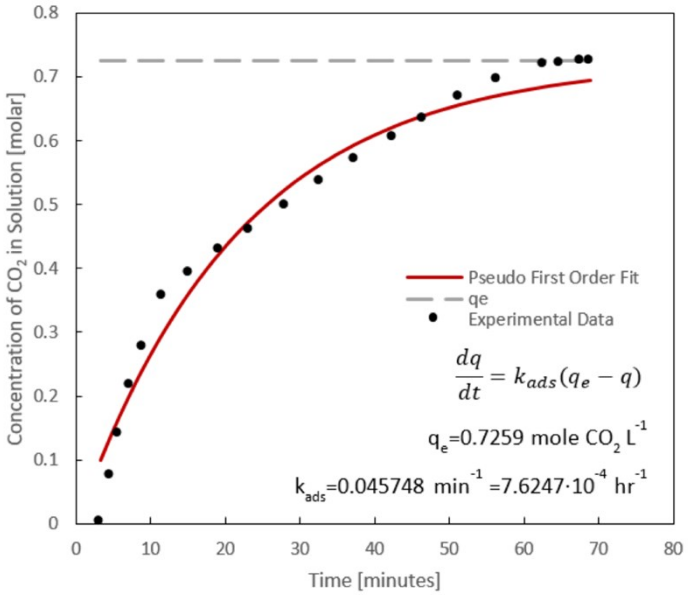

Figure S2. Experimental data from Yoo *et al.*[11] measuring gaseous CO_2 adsorption into a three percent sodium hydroxide solution fit to a pseudo-first order model to obtain an adsorption rate constant.

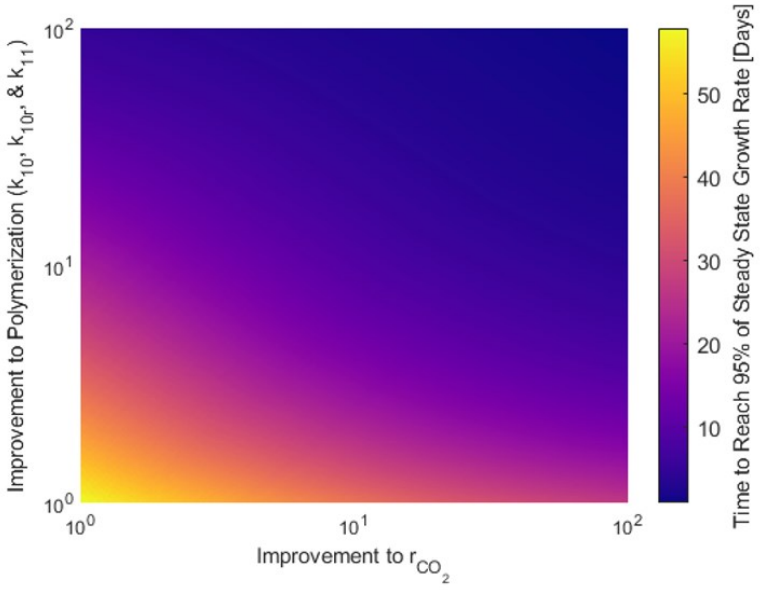

Figure S3. Time for the Carbon Fixing Material to reach 95% of its steady-state, maximum growth rate. The lower left-hand corner represents the value for the case study presented, with no improvement to polymerization kinetics or formaldehyde production rate.

Preliminary Techno-Economic Analysis of Carbon Fixing Materials:

One application of carbon fixing materials is their use to extend the lifetime of industrial or domestic coatings or other materials. Compared to traditional materials which inevitably weather and degrade upon exposure to sunlight, water, oxygen, and other contaminants—carbon fixing materials which gain mass could do the opposite, strengthening and reinforcing over time. To estimate impact on life space of traditional coatings through incorporation of a carbon fixing component within, the following calculation was performed. Assuming a constant net rate of natural coating mass degradation, the life time of this material is defined as the period before a certain fraction of coating is degraded. Incorporating a carbon fixing component that also produces a constant net rate of mass growth and repair, the lifetime of the coating is extended. The new lifetime of the material is then a function of the rates of natural mass gain to degradation—which is plotted in Figure S4.

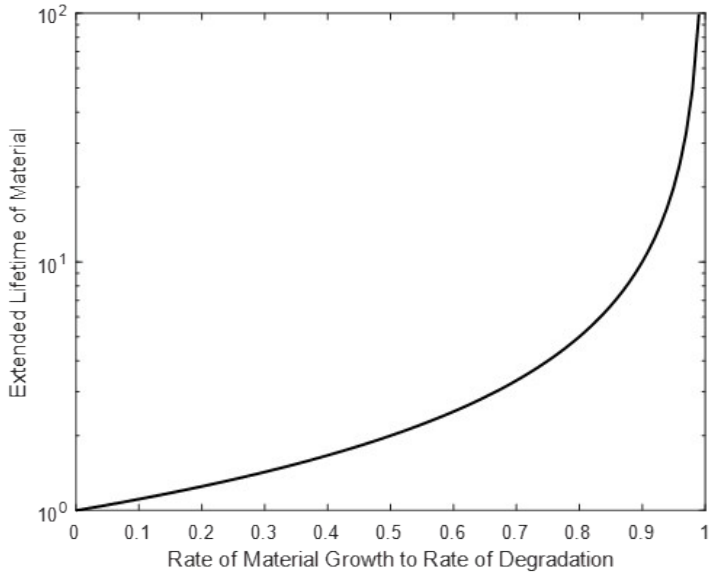

Figure S4. Self-healing characteristic of CFMs makes them promising candidates in applications where the overtime degradation of materials is a concern. Depending on the CFM growth rate, the average life-time of materials can be extended to various degrees.

As seen, any additional material growth may enhance the lifetime of a coating—with a doubling of lifetime when the material growth rate is half that of the degradation rate. The lifetime may be extended by an order of magnitude if the growth rate approaches 90% of the degradation rate.

The potential economic impact of the increased lifetime of such coatings is explored in Figure S5 for a variety of differing coating systems: epoxy[22], metallized[22], and various coatings for offshore applications[23].

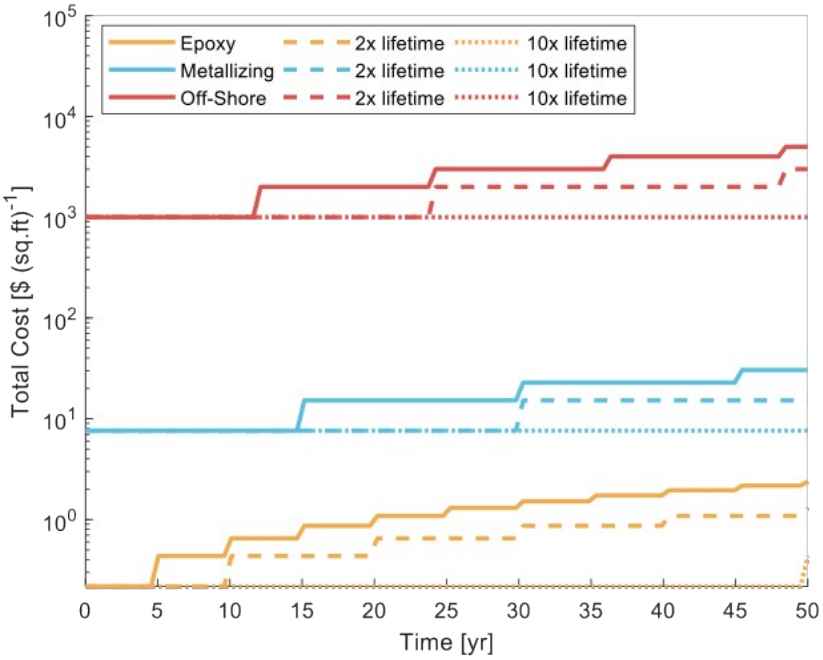

Figure S5. Economic analysis of the hypothetical self-healing CFM coatings: by applying CFMs on top of conventional coatings, their lifetimes can be extended by multiple factors depending on the relative growth rate of CFM to coating degradation rate. The effect of the presumed extended life-time on the total cost of coatings in their life cycles (including the initial coating, maintenance, repair, and reapplying) varies from a few dollar/sq.ft in epoxy-based coating to a few thousand dollars/sq.ft in off-shore coatings.

Further Discussion on Future Outlook of CFM:

The timescale and chemical conditions for carbon fixing materials in the environment can vary significantly from those used for the experimental study of CO_2 adsorbents and photocatalyst in the laboratory. Many experimental and chemical approaches to successful CO_2 photoreduction may not be directly applicable for incorporation into carbon fixing material. A more exhaustive quantification of probably chemical species produced during CO_2 photoreduction, and experimental conditions representative of the ambient environment where carbon fixing material are to function are all necessary to facilitate the development of improved systems. This is a break from many experimental procedures where the liquid-phase reduction products such as formate, formaldehyde, and methanol are either not reported as being observed, or no mention of effort to detect them is present. This may be due to the ease of analytical methods such as gas chromatography being common for quantification of carbon monoxide and methane. Such detection methods become increasingly laborious when the liquid-phase need be sampled—especially since formaldehyde and formate have traditionally required derivatization for detection at low concentrations with gas chromatography.

As presented, the catalytic activity of the cobalt-supported TiO_2 photocatalyst within the saturated CO_2 system is on the order of 10 μmol gcat-1 hr-1. However higher activity CO_2 photoreduction

catalysts have been reported, with several reaching activities on the order of 1,000 μmol gcat-1 hr-1 or greater[24],[25],[26],[27], [28], obtained at room temperature and 1 atm of CO_2 or higher . However, few report on the production of products besides carbon monoxide or methane. Incorporation of an improved photocatalyst within a carbon fixing material is then currently not limited necessarily by activity, but selectivity, as it remains unknown whether formaldehyde (or another product) is produced as an intermediate in appreciable amounts. In the example explored in this work, the polymerization pathway from formaldehyde to polyoxymethylene can effectively incorporates 100% of photocatalytically converted CO_2 due to the fast rate of formaldehyde hydration. In more realistic systems where this is not the case, a possible solution could be to shuttle formaldehyde, or any other product intermediate in the photocatalytic conversion pathway, using of a selective adsorbent. This would allow for higher yield and selectivity[29],[30]. A more complete characterization of the production distribution obtained by photocatalytic reduction of CO_2 will facilitate both the understanding of the catalytic system, as well as its potential for incorporation into a carbon fixing material.

It is both an opportunity and a limitation that the timescale and chemical reaction conditions for carbon fixing materials in the environment can vary significantly from those used for the experimental study of CO_2 adsorbents and photocatalyst in the laboratory or used in industry. Many experimental and chemical approaches to successful CO_2 photoreduction may not be directly applicable for incorporation into carbon fixing material, providing an opportunity to discover catalysts under previously unexplored conditions. The use of consumable hole scavenging agents—such as isopropanol, sodium sulfate, and hydrogen peroxide—to enhance photocatalytic efficiency is a common practice in the study of CO_2 photocatalytic reduction[31]. These approaches may not directly support carbon fixing material as presented here, which we envision as exhibiting sustained growth with persistent catalytic activity even after exhaustion of any preloaded components. Second, physical adsorbent systems such as metal-organic frameworks will require the investigation of their adsorption capacity at ambient atmospheric condition—hundreds of parts per million of CO_2. Specifically, their selectivity of adsorption of CO_2 to nitrogen and their capacity need be evaluated under these conditions—where nitrogen is nearly 2,000 times relatively more abundant than CO2, and adsorption capacities of the gas can be a fraction of that measured under an atmosphere of CO_2[32]. The carbon fixing material application may allow materials with limited thermal stability to be used, since high temperatures are not expected. Lastly, the photocatalytic system employed within a carbon fixing material needs to maintain its activity over long periods of time. This encourages the investigation of any photocatalytic system at length and reuse. Additionally, less robust classes of photocatalysts such as those containing biological components such as proteins may need stabilization before incorporation into carbon fixing materials [33],[34].

Table S2. Most relevant mass transfer and reaction kinetics model of CO_2 adsorption

Article	**Summary**

Modeling CO_2 Capture in Amine Solvents: Prediction of Performance and Insights on Limiting Phenomena [35]	In this study, a model of absorption and stripping column for post-combustion CO_2 capture in amine solvents is developed using the rate of mass transfer and thermodynamics of vapor-liquid equilibria.
Moving Beyond Adsorption Capacity in Design of Adsorbents for CO_2 Capture from Ultradilute Feeds: Kinetics of CO_2 Adsorption in Materials with Stepped Isotherms [36]	Moving away from equilibrium adsorption analysis, this study develops a combined mass transfer and adsorption kinetic model for CO_2 adsorption on amine-functionalized MOFs.
Bayesian Inference of Aqueous Mineral Carbonation Kinetics for Carbon Capture and Utilization [37]	This study develops mathematical model for aqueous mineral carbonation kinetics for carbon capture and utilization, using mass transfer between gas and liquid phases, solid dissolution and ionization reactions.
Development of a Rigorous Modeling Framework for Solvent-Based CO_2 Capture. 1. Hydraulic and Mass Transfer Models and Their Uncertainty Quantification [38]	This study develops mass transfer, column hydraulics and reaction kinetics model for post-combustion CO_2 capture through a process model of MEA-H_2O-CO_2 system.

References

1. Varma, A.; Morbidelli, M.; Wu, H., *Parametric Sensitivity in Chemical Systems*. Cambridge University Pess: Cambridge, UK, 1999.
2. Ordonez, M. C.; Raftery, J. P.; Jaladi, T.; Chen, X. H.; Kao, K.; Karim, M. N., Modelling of batch kinetics of aerobic carotenoid production using Saccharomyces cerevisiae. *Biochemical Engineering Journal* **2016,** *114*, 229-239.
3. Winkelman, J. G. M.; Ottens, M.; Beenackers, A., The kinetics of the dehydration of methylene glycol. *Chemical Engineering Science* **2000,** *55* (11), 2065-2071.
4. Ott, M.; Fischer, H. H.; Maiwald, M.; Albert, K.; Hasse, H., Kinetics of oligomerization reactions in formaldehyde solutions: NMR experiments up to 373 K and thermodynamically consistent model. *Chemical Engineering and Processing-Process Intensification* **2005,** *44* (6), 653-660.
5. Kuhnert, C.; Albert, M.; Breyer, S.; Hahnenstein, I.; Hasse, H.; Maurer, G., Phase equilibrium in formaldehyde containing multicomponent mixtures: Experimental results for fluid phase equilibria of (formaldehyde plus (water or methanol) plus methylal)) and (formaldehyde plus water plus methanol plus methylal) and comparison with predictions. *Industrial & Engineering Chemistry Research* **2006,** *45* (14), 5155-5164.
6. Yin, L. Y.; Hu, Y. F.; Zhang, X. M.; Qi, J. G.; Ma, W. T., The salt effect on the yields of trioxane in reaction solution and in distillate. *Rsc Advances* **2015,** *5* (47), 37697-37702.

7. Zhang, X. M.; Hu, Y. F.; Ma, W. T., A model for the reaction kinetics of main and side reactions during the industrial production of trioxane, and its applications. *Journal of Chemical Technology and Biotechnology* **2018,** *93* (8), 2111-2117.
8. Kua, J.; Avila, J. E.; Lee, C. G.; Smith, W. D., Mapping the Kinetic and Thermodynamic Landscape of Formaldehyde Oligomerization under Neutral Conditions. *Journal of Physical Chemistry A* **2013,** *117* (47), 12658-12667.
9. Shieh, Y. T.; Chen, S. A., Kinetics and mechanism of the cationic polymerization of trioxane. I. Crystallization during polymerization. *Journal of Polymer Science Part a-Polymer Chemistry* **1999,** *37* (4), 483-492.
10. Hoffmann, M.; Bizzarri, C.; Leitner, W.; Muller, T. E., Reaction pathways at the initial steps of trioxane polymerisation. *Catalysis Science & Technology* **2018,** *8* (21), 5594-5603.
11. Yoo, M.; Han, S.-J.; Wee, J.-H., Carbon dioxide capture capacity of sodium hydroxide aqueous solution. *Journal of Environmental Management* **2013,** *114*, 512-519.
12. Ji, Y.; Luo, Y., Theoretical Study on the Mechanism of Photoreduction of CO2 to CH4 on the Anatase TiO2 (101) Surface. *ACS Catalysis* **2016,** *6* (3), 2018-2025.
13. Kortlever, R.; Shen, J.; Schouten, K. J. P.; Calle-Vallejo, F.; Koper, M. T., Catalysts and reaction pathways for the electrochemical reduction of carbon dioxide. *The journal of physical chemistry letters* **2015,** *6* (20), 4073-4082.
14. Kuhl, K. P.; Cave, E. R.; Abram, D. N.; Jaramillo, T. F., New insights into the electrochemical reduction of carbon dioxide on metallic copper surfaces. *Energy & Environmental Science* **2012,** *5* (5), 7050-7059.
15. Hatsukade, T.; Kuhl, K. P.; Cave, E. R.; Abram, D. N.; Jaramillo, T. F., Insights into the electrocatalytic reduction of CO 2 on metallic silver surfaces. *Physical Chemistry Chemical Physics* **2014,** *16* (27), 13814-13819.
16. He, H.; Zapol, P.; Curtiss, L. A., Computational screening of dopants for photocatalytic two-electron reduction of CO2 on anatase (101) surfaces. *Energy & Environmental Science* **2012,** *5* (3), 6196-6205.
17. Cheng, T.; Xiao, H.; Goddard III, W. A., Free-energy barriers and reaction mechanisms for the electrochemical reduction of CO on the Cu (100) surface, including multiple layers of explicit solvent at pH 0. *The journal of physical chemistry letters* **2015,** *6* (23), 4767-4773.
18. Genovese, C.; Ampelli, C.; Perathoner, S.; Centi, G., Mechanism of C–C bond formation in the electrocatalytic reduction of CO 2 to acetic acid. A challenging reaction to use renewable energy with chemistry. *Green Chemistry* **2017,** *19* (10), 2406-2415.
19. Garza, A. J.; Bell, A. T.; Head-Gordon, M., Mechanism of CO2 reduction at copper surfaces: pathways to C2 products. *ACS Catalysis* **2018,** *8* (2), 1490-1499.
20. Goodpaster, J. D.; Bell, A. T.; Head-Gordon, M., Identification of possible pathways for C–C bond formation during electrochemical reduction of CO2: new theoretical insights from an improved electrochemical model. *The journal of physical chemistry letters* **2016,** *7* (8), 1471-1477.
21. Zheng, Y.; Vasileff, A.; Zhou, X.; Jiao, Y.; Jaroniec, M.; Qiao, S.-Z., Understanding the roadmap for electrochemical reduction of CO2 to multi-carbon oxygenates and hydrocarbons on copper-based catalysts. *Journal of the American Chemical Society* **2019,** *141* (19), 7646-7659.
22. Helsel, J. L. a. L. R., Expected service life and cost considerations for maintenance and new construction protective coating work. *NACE - International Corrosion Conference Series* **2016,** *3* (08279), 2118--2132.

23. Price, S. J. a. F. R. B., Corrosion protection systems and fatigue corrosion in offshore wind structures: Current status and future perspectives. *Coatings* **2017,** *7* (2), 1--51.
24. Lingampalli, S. R.; Ayyub, M. M.; Rao, C. N. R., Recent Progress in the Photocatalytic Reduction of Carbon Dioxide. *Acs Omega* **2017,** *2* (6), 2740-2748.
25. Yuan, Y. P.; Cao, S. W.; Liao, Y. S.; Yin, L. S.; Xue, C., Red phosphor/g-C3N4 heterojunction with enhanced photocatalytic activities for solar fuels production. *Applied Catalysis B-Environmental* **2013,** *140*, 164-168.
26. Zhang, X. J.; Han, F.; Shi, B.; Farsinezhad, S.; Dechaine, G. P.; Shankar, K., Photocatalytic Conversion of Diluted CO2 into Light Hydrocarbons Using Periodically Modulated Multiwalled Nanotube Arrays. *Angewandte Chemie-International Edition* **2012,** *51* (51), 12732-12735.
27. Neatu, S.; Macia-Agullo, J. A.; Concepcion, P.; Garcia, H., Gold-Copper Nanoalloys Supported on TiO2 as Photocatalysts for CO2 Reduction by Water. *Journal of the American Chemical Society* **2014,** *136* (45), 15969-15976.
28. Zhang, Z. Y.; Wang, Z.; Cao, S. W.; Xue, C., Au/Pt Nanoparticle-Decorated TiO2 Nanofibers with Plasmon-Enhanced Photocatalytic Activities for Solar-to-Fuel Conversion. *Journal of Physical Chemistry C* **2013,** *117* (49), 25939-25947.
29. Bellat, J. P.; Weber, G.; Bezverkhyy, I.; Lamonier, J. F., Selective adsorption of formaldehyde and water vapors in NaY and NaX zeolites. *Microporous and Mesoporous Materials* **2019,** *288*.
30. Jin, Z.; Wang, L.; Hu, Q. X.; Zhang, L.; Xu, S. D.; Dong, X.; Gao, X. H.; Ma, R. Y.; Meng, X. J.; Xiao, F. S., Hydrophobic Zeolite Containing Titania Particles as Wettability-Selective Catalyst for Formaldehyde Removal. *Acs Catalysis* **2018,** *8* (6), 5250-5254.
31. Tan, J. Z. Y.; Maroto-Valer, M. M., A review of nanostructured non-titania photocatalysts and hole scavenging agents for CO2 photoreduction processes. *Journal of Materials Chemistry A* **2019,** *7* (16), 9368-9385.
32. Hu, Z.; Wang, Y.; Shah, B. B.; Zhao, D., CO2 Capture in Metal-Organic Framework Adsorbents: An Engineering Perspective. *Advanced Sustainable Systems* **2019,** *3* (1).
33. Yadav, R. K.; Oh, G. H.; Park, N.-J.; Kumar, A.; Kong, K.-j.; Baeg, J.-O., Highly Selective Solar-Driven Methanol from CO2 by a Photocatalyst/Biocatalyst Integrated System. *Journal of the American Chemical Society* **2014,** *136* (48), 16728-16731.
34. Yadav, R. K.; Baeg, J.-O.; Kumar, A.; Kong, K.-j.; Oh, G. H.; Park, N.-J., Graphene-BODIPY as a photocatalyst in the photocatalytic-biocatalytic coupled system for solar fuel production from CO2. *Journal of Materials Chemistry A* **2014,** *2* (14), 5068-5076.
35. Neveux, T.; Le Moullec, Y.; Corriou, J. P.; Favre, E., Modeling CO2 Capture in Amine Solvents: Prediction of Performance and Insights on Limiting Phenomena. *Industrial & Engineering Chemistry Research* **2013,** *52* (11), 4266-4279.
36. Darunte, L. A.; Sen, T.; Bhawanani, C.; Walton, K. S.; Sholl, D. S.; Realff, M. J.; Jones, C. W., Moving Beyond Adsorption Capacity in Design of Adsorbents for CO2 Capture from Ultradilute Feeds: Kinetics of CO2 Adsorption in Materials with Stepped Isotherms. *Industrial & Engineering Chemistry Research* **2019,** *58* (1), 366-377.
37. Na, J.; Park, S.; Bak, J. H.; Kim, M.; Lee, D.; Yoo, Y.; Kim, I.; Park, J.; Lee, U.; Lee, J. M., Bayesian Inference of Aqueous Mineral Carbonation Kinetics for Carbon Capture and Utilization. *Industrial & Engineering Chemistry Research* **2019,** *58* (19), 8246-8259.

38. Chinen, A. S.; Morgan, J. C.; Omell, B.; Bhattacharyya, D.; Tong, C.; Miller, D. C., Development of a Rigorous Modeling Framework for Solvent-Based CO2 Capture. 1. Hydraulic and Mass Transfer Models and Their Uncertainty Quantification. *Industrial & Engineering Chemistry Research* **2018,** *57* (31), 10448-10463.